

**Jelena Svorcan**

Assistant Professor  
University of Belgrade  
Faculty of Mechanical Engineering

**Zorana Trivković**

Research Associate  
University of Belgrade  
Faculty of Mechanical Engineering

**Toni Ivanov**

Assistant Professor  
University of Belgrade  
Faculty of Mechanical Engineering

**Marija Baltić**

Research Associate  
University of Belgrade  
Faculty of Mechanical Engineering

**Ognjen Peković**

Assistant Professor  
University of Belgrade  
Faculty of Mechanical Engineering

# Multi-objective Constrained Optimizations of VAWT Composite Blades Based on FEM and PSO

*Vertical-axis wind turbines (VAWTs) are attractive tools for wind energy extraction particularly suitable for small consumers or off-grid areas. Although their geometry is simple (here, rectangular blade of constant airfoil is assumed), aerodynamic analysis may be quite complex. Computational fluid dynamics (CFD) approach is employed for the estimation of rotor aerodynamic performances. This paper provides a review of possible multi-objective optimization strategies for the design of small-scale VAWT laminate blades in terms of its main structural parameters: ply-order and ply-number. Numerous structural analyses of the composite turbine blades were performed by finite element method (FEM). Multi-criteria constrained optimizations, by an evolutionary method – particle swarm optimization (PSO), were performed with respect to blade total mass, maximum blade tip deflection under static loading, computed natural frequencies and failure index along the blade. By combining different input and output parameters (cost functions and constraints) a large variety of feasible solutions can be achieved.*

**Keywords:** VAWT, Blade, CFD, Laminate, FEM, Multi-objective PSO.

## 1. INTRODUCTION

In accordance with the current industrial and economic trends and the appeal of renewable energy sources, wind turbine blades present one of the contemporary topics of scientific and engineering research [1, 2]. The work presented in [3] gives a good overview of the complete wind turbine rotor blades development process and accentuates the importance of a synchronous coordination between several (equally important) research areas: design (aerodynamic and structural), regulations and standards, applied materials, manufacturing technologies and verification testing. It also promotes the use of various contemporary engineering techniques such as: design improvement, optimization, use of novel materials, etc.

Throughout the past century several different wind turbine concepts have been tried, usually categorized according to the direction of their rotational axis. Somewhat less known, but also interesting and promising type is a vertical-axis wind turbine (VAWT) of a geometrically much simpler shape than a conventional horizontal-axis wind turbine (HAWT). The distinctive characteristics of VAWTs include: simple design, low production cost, operability in “dirty” winds (of changeable intensity and direction), as well as somewhat lower efficiency than HAWTs. Interesting work on the possible improvement of their aerodynamic performances can be found in [4, 5].

The subject of this investigation, a Darrieus straight-bladed VAWT, contains blades of constant chord and airfoil along their lengths. The research motive is the improvement of its structural design which could ultimately

lead to the reduced blade mass and cost, prolonged working life, reduced loading to the tower, etc. (numerous advantages) while preserving structural reliability and integrity. Given that contemporary wind turbine blades are mostly composite [1-13], particularly in small-scale constructions, the paper investigates the possibilities of applying a multi-objective optimization approach to the blade structural design.

Optimization of the blade composite lay-up and ply orientations can be done numerically, by coupling a finite element (FE) solver with a multi-objective optimization method. Given the complexity and nonlinearity of both cost-functions and imposed constraints, usually, one of the evolutionary, heuristic methods is applied [8-12]. This methodology can be implemented to HAWTs and VAWTs, as well as other mechanical parts/systems. Albanesi et al. [7] performed optimizations of HAWT blade by genetic algorithm (GA), Wang et al. [9] dealt with large VAWT blade also by GA, while Chen et al. [10] used a particle swarm optimization (PSO) method.

This research paper communicates several different multi-objective PSO strategies with integer design variables. It is arranged in the following fashion: the following section describes the initial blade geometry after which the estimation of its aerodynamic performances by computational fluid dynamics (CFD) approach is given. Section “Structural model” clearly explains the assumed blade laminate structure, with its parameterization and optimization algorithm described in detail in the following section. Finally, the gained experiences and results, discussion and conclusions are listed in the end.

## 2. GEOMETRIC MODEL

The starting, reference blade model designed for a straight small-scale Darrieus VAWT of nominal power  $P_{\text{nom}} = 500$  W is presented in Fig. 1. Its main characteristics and dimensions are: the number of blades  $N_b =$

Received: March 2019, Accepted: May 2019

Correspondence to: Dr Jelena Svorcan  
Faculty of Mechanical Engineering,  
Kraljice Marije 16, 11120 Belgrade 35, Serbia  
E-mail: jsvorcan@mas.bg.ac.rs

doi:10.5937/fmet1904887S

© Faculty of Mechanical Engineering, Belgrade. All rights reserved

FME Transactions (2019) 47, 887-893 887

3, turbine radius  $R = 1.5$  m (diameter  $D = 3.0$  m), blade chord  $c = 15$  cm resulting in rotor solidity  $\sigma = cN_b/D = 0.15$  and blade length  $L = 1$  m. Reference area is defined as  $A = DL = 3$  m<sup>2</sup>. The blade is straight and of constant symmetric airfoil NACA 0018 along its length. Nominal rotor angular velocity  $\omega = 200$  RPM is kept constant and results in the period  $T = 0.3$  s. Designed wind speed at which the turbine is expected to generate approximately 500 W is  $V_o = 10$  m/s.

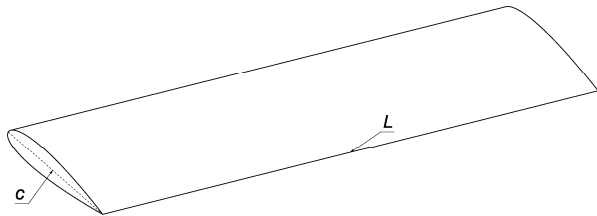


Figure 1. Outer blade geometry

### 3. FLOW COMPUTATION

Aerodynamic performances of the wind turbine rotor are computed by finite volume method in the commercial software package ANSYS FLUENT [14]. Fundamental equations governing the transient, incompressible, turbulent fluid flow are solved in integral form and closed by a two-equation  $k-\omega$  SST turbulence model [15].

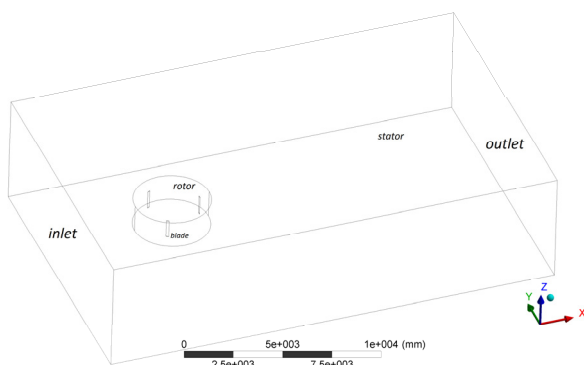


Figure 2. Parts and boundaries of the computational domain.

Since the flow in question is complex and asymmetric with flow phenomena being present, one of the computationally most expensive numerical approaches, “Sliding mesh”, had to be employed. With this concept, the computational domain has to comprise at least two independent zones that move relevant to each other. As illustrated in Fig. 2, the wind turbine rotor consists of 3 isolated blades. Computational domain around the blades is split into two adjacent zones: inner, rotational cylinder – *rotor*, and outer, stationary block – *stator*. The radius of the rotating part is  $1.33R$ , while its height extends  $\pm 0.75L$  in the vertical direction. The limits of the outer domain are:  $-3R$  before and  $11R$  after the rotational axis along the longitudinal  $x$ -axis,  $\pm 4R$  along the lateral  $y$ -axis and  $\pm 2L$  along the vertical  $z$ -axis.

In order to assure the independence of results from the computational grid, mesh convergence study was performed. The final mesh, used throughout this study, is hybrid unstructured, containing approximately 3.2

million cells. Biased cell size functions are defined along the blade edges, in both chord- and span-wise directions. Inner, rotor zone is more refined than the outer stator. Cells grow larger towards the outer boundaries, Fig. 3. Twenty layers of prismatic cells with growth rate  $q = 1.2$  encompass the blades. First layer thickness is  $y_1 = 0.05$  mm resulting in dimensionless distance from the wall  $y^+ < 5$ .

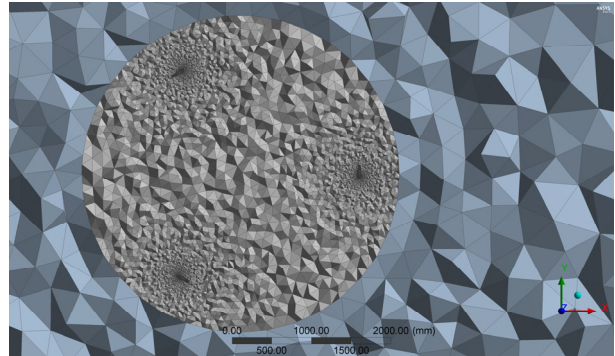


Figure 3. Cross-section of the computational grid with two distinct zones

Numerical simulations for incompressible, viscous fluid were performed in ANSYS FLUENT. Unsteady Reynolds-averaged Navier-Stokes equations were closed by a two-equation  $k-\omega$  SST turbulence model, a combination of standard  $k-\omega$  model near the walls and  $k-\epsilon$  in the outer layer [15]. Fluid, air, was considered as incompressible gas of constant dynamic viscosity (this is an adequate assumption due to small wind velocities).

Boundary conditions are defined as follows. Undisturbed wind speed  $V_o$  ranging from 6 m/s to 18 m/s together with the necessary turbulent quantities – intensity  $t = 5\%$  and relative turbulent viscosity  $\nu_t/\nu = 10$  are defined at the inlet surfaces while atmospheric pressure is set at the outlet. Rotational zone motion (of constant angular velocity  $\omega$  for all flow cases) is assigned to the rotor, while blades are considered as no-slip rotational walls.

For solving the flow equations pressure-based solver with SIMPLEC pressure-velocity coupling is used. All spatial derivatives are approximated by 2nd order schemes, while temporal discretization is of the 1st order. Time step,  $\Delta t = T/72$ , corresponds to  $5^\circ$  angular increment. Ten iterations are performed per each time-step. Each flow case simulation lasted at least 5 revolutions until quasi-convergence of aerodynamic coefficients was achieved.

Although all recorded quantities are periodic, an example in the form of generated torque is illustrated in Fig. 4, it is possible to evaluate global aerodynamic performances of the wind turbine by using the mean values of aerodynamic torque. Figure 5 shows both averaged power coefficient curve with respect to tip-speed ratio  $C_p(\lambda)$ , as well as the estimation of the wind turbine mechanical power with respect to wind speed  $P(V_o)$ . It seems that maximal power coefficient  $C_{pmax} = 0.2633$  can be achieved at the optimal working regime  $\lambda_{opt} = 2.86$  which corresponds to the wind speed  $V_o = 11$  m/s. Additionally, due to the shape of the power curve, very similar power coefficients are accomplished at  $V_o = 10$  m/s and  $V_o = 12$  m/s.

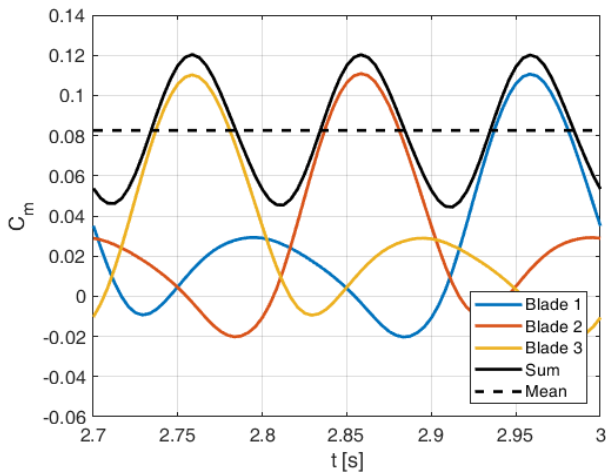


Figure 4. Torque coefficients from each blade, total sum and averaged value at the optimal working regime

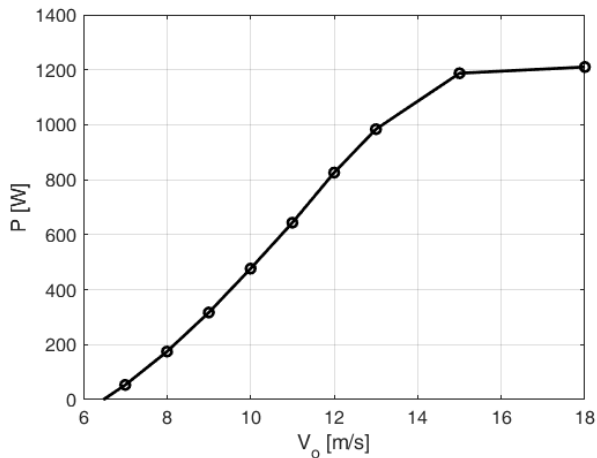
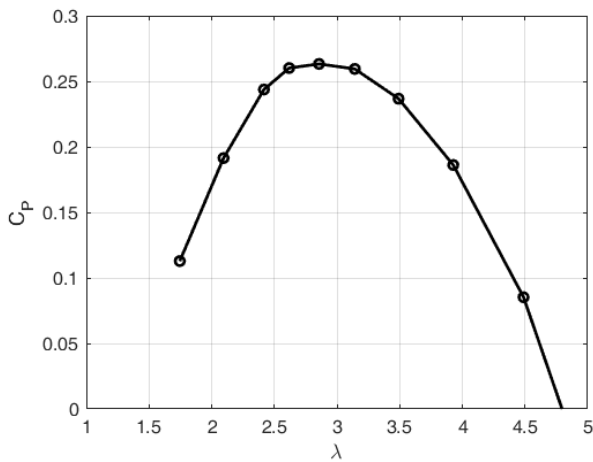


Figure 5. Computed aerodynamic performances of the designed VAWT

Computed force variations acting on a single blade during one revolution for the several different working regimes (wind speeds) are depicted in Fig. 6. The differences in aerodynamic contributions in the “upwind” ( $-90^\circ \leq \theta \leq 90^\circ$ ) and “downwind” ( $90^\circ \leq \theta \leq 270^\circ$ ) part of the rotor, which present the main dynamic, cyclic loading these wind turbines are exposed to, are significant and apparent.

The obtained maximum values of normal and tangential forces at wind speed  $V_o = 18$  m/s were later used as the load input for the structural computations and blade dimensioning.

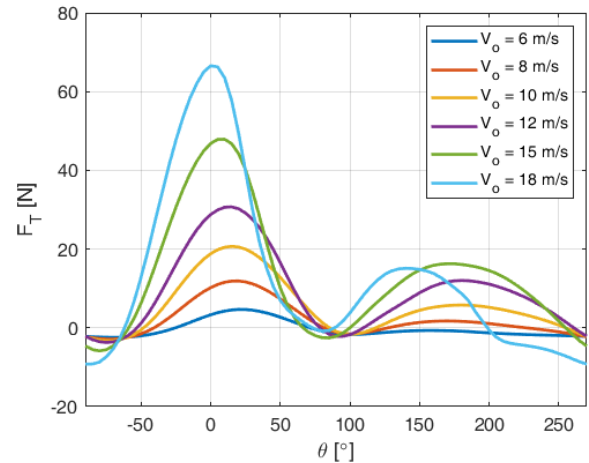
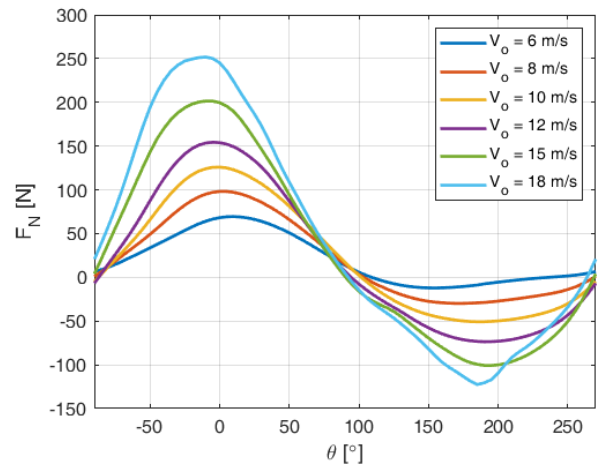


Figure 6. Computed forces acting on the blade during a revolution at different wind speeds

#### 4. STRUCTURAL MODEL

Simplified blade model, consisting solely of the upper and lower outer surfaces and a single shear web located at the first quarter of the airfoil, is assumed as a symmetric Epoxy E-Glass laminate consisting of 55% unidirectional plies organized in the following sequence  $[(\theta_1)_{n1} / (\theta_2)_{n2} / (\theta_3)_{n3} / (\theta_2)_{n2} / (\theta_2)_{n2} / (\theta_1)_{n1}]$ , where all six design variables  $n_1, \theta_1, n_2, \theta_2, n_3$  and  $\theta_3$  are integers. Material properties are listed in Table 1.

Table 1. Material (Epoxy E-Glass Prepreg) properties

Property	Unit	Value
$\rho$	(g/cm <sup>3</sup> )	2.0
$E_1, E_2$	(GPa)	45.0, 10.0
$G_{12}$	(GPa)	5.0
$\nu_{12}$		0.3
$F_{1t}, F_{1c}$	(MPa)	1100.0, -675.0
$F_{2t}, F_{2c}$	(MPa)	35.0, -120.0
$F_6$	(MPa)	80.0

Generated finite element meshes consist of approximately 4500 quadrilateral shell elements, Fig. 7. Due to its small size, the blade is only clamped at the middle cross-section. Uniformly distributed aerodynamic, inertial and gravitational loads are applied along the blade.

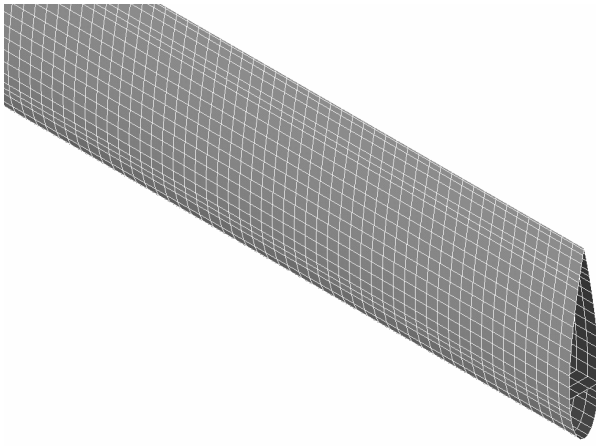


Figure 7. Part of the finite element mesh

## 5. OPTIMIZATION

Given the complexity of the problem that involves non-linear objective functions, inequality constraints and various discrete design variables, the optimization of the blade structure was performed by a non-deterministic particle swarm method [16] inspired by the behavior of a group of individuals in the search for food. Ever since its formulation in 1995, it has been excessively used for its algorithm (and code) simplicity and rapid convergence.

The current position of each individual particle in the design space is characterized by the following vector  $[n_1 \theta_1 n_2 \theta_2 n_3 \theta_3]$ , where  $n_i$  denotes ply number and  $\theta_i$  its orientation with respect to the longitudinal  $x$ -axis of the blade. Thickness of a single ply is assumed to be  $dt = 0.1$  mm, resulting in the total laminate thickness  $t = (2n_1 + 2n_2 + n_3)dt$ . Minimum ply number is 5. From the design space boundaries, listed in Table 2, it can be concluded that the total number of possible blade structure designs goes beyond 1 million. In every iteration, every particle moves through the design space by the velocity vector that is computed partially randomly and takes into account both “cognitive” and “social” influence.

Table 2. Design space

Variable	$n_i$	$\theta_i$ (°)
Min	1	0
Max	15	90
Increment	1	15
Set size	15	7

Two-criterion assessment in PSO was achieved by forming an archive of non-dominated Pareto solutions. The chosen cost-functions are minimum blade mass  $\min(m)$  and minimal blade tip deflection  $\min(u_{tip})$ :

$$\min(m) \square \min(u_{tip})$$

subject to:

$$I_{fail} \leq 1,$$

$$|nv_{nom} - v_i| \geq 0.5 \text{ Hz}, i \in [1, 5], n \in [1, 3].$$

The imposed constraints are meant to assure long and reliable blade operation, both static and dynamic. Therefore, they include: the satisfactory value of Tsai-Wu failure index  $I_{fail}$  along the whole blade and sufficient difference between the first 5 natural frequencies  $v_i$  and the integer multiplies of the nominal rotor angular frequency  $nv_{nom}$ . Here, minimal frequency difference

was set to  $\Delta v = 0.5$  Hz which corresponds to 15% of the nominal rotor angular frequency. The large value of the safety factor is adopted since discrepancies between the actual and modeled geometry can be expected. Modal analysis of rotational composite structures is very important for their safe and steady functioning. Similarly to [13], the eigenvalue extraction was performed by the Lanczos method.

Likewise, the goals and constraints of the performed three-criterion PSO of the blade structure are:

$$\min(m) \square \min(u_{tip}) \square \max(|nv_{nom} - v_i|)$$

subject to:

$$I_{fail} \leq 1.$$

Considering the swarm organization, total number of particles was 100 while the number of iterations was 30 (plus the initial step). Results convergence was assured by repeating the optimization procedures several times and by varying the swarm size and number of computational steps.

## 6. RESULTS AND DISCUSSION

The distinctiveness of a multi-objective optimization, in comparison with the classic single-objective, is that its outcome is not a single design, but rather a set of optimal designs from which it is possible to choose. The obtained 2D and 3D Pareto frontiers (sets of optimal solutions) together with all computed particles are presented in Figs. 8 and 9 respectively.

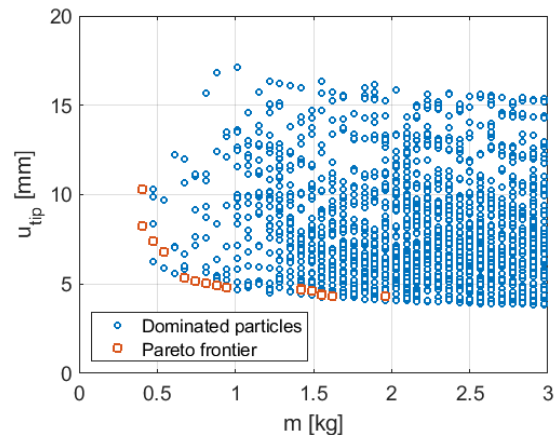


Figure 8. 2D Pareto frontier

For 2D optimization and 2D Pareto frontier, the total number of plies varies from 6 to 29 resulting in blade mass lower bound of 0.41 kg to maximum 1.96 kg. Corresponding blade tip deflections range from 10.31 mm to 4.33 mm. Furthermore, the conducted optimization procedure demonstrates that while the outer ( $n_1, \theta_1$ ) and inner layer ( $n_3, \theta_3$ ) may be aligned at angles such as  $0^\circ$  and  $15^\circ$  but also  $75^\circ$  and  $90^\circ$ , the middle layer can exclusively be oriented at  $0^\circ$ . Interestingly, the angle of  $45^\circ$  is not present in any layer. All optimal designs satisfy the imposed constraints.

In case both selected criteria are considered equally important, one way to select the optimal solution may be by choosing the particle closest to the point (0,0) in normalized coordinates. In this 2D example, the optimal design chosen for further analysis and comparison is defined by  $[1, 90^\circ, 1, 0^\circ, 4, 0^\circ]$  and named model 1 for the remainder of the study.

Performed 3-criterion PSO resulted in a Pareto frontier of a saddle-like shape, Fig. 9. Furthermore, more insight into the relations between the selected criteria was achieved. Also, some differences between the two optimization procedures exist. First of all, 3D PSO resulted in somewhat heavier blades. Attained blade mass values range from 0.61 kg to 2.84 kg, i.e. total number of plies varies between 9 and 42. On the other hand, additionally strengthened blade structure also implies lower tip deflections, with values ranging between 4.34 mm and 8.47 mm. Differences in inner structure are also notable. While the inner and middle layers can be oriented at various angles, the outer, symmetric layer is now dominantly aligned along the longitudinal  $x$ -axis (at  $0^\circ$ ). The optimal solution, named model 2, chosen for supplementary examination is defined by  $[3, 0^\circ, 1, 90^\circ, 1, 60^\circ]$ .

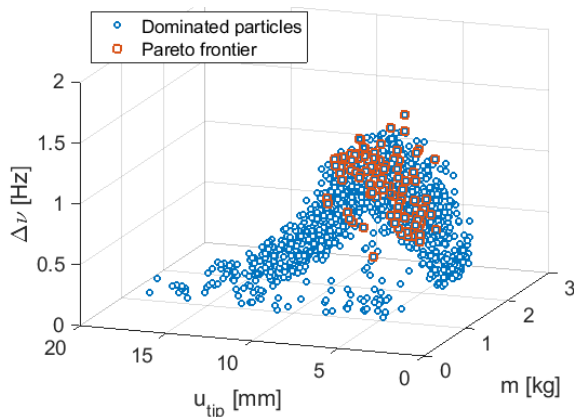


Figure 9. 3D Pareto frontier

Computed blade displacements under static (aerodynamic, gravitational and inertial) loading are presented in Fig. 10 where red color corresponds to maximal values and blue to 0 (at the middle of the blades, where they are clamped).

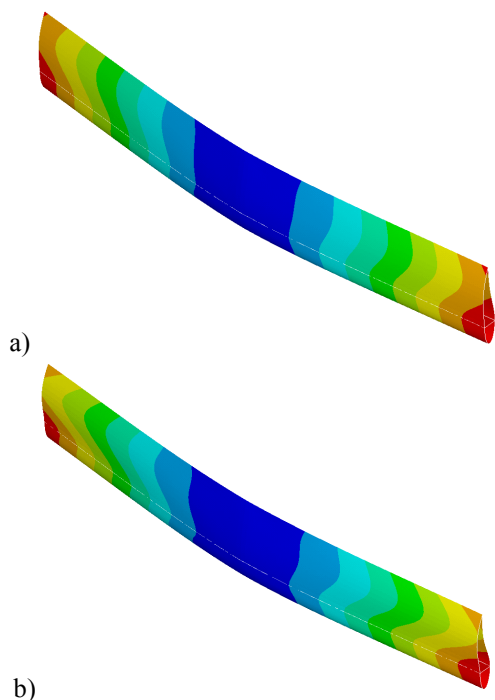


Figure 10. Computed blade displacements under static loading for: a) model 1, b) model 2

The differences in computed mass and tip displacement of the two structural designs, model 1 and model 2, including the maximum failure index along the blade and the first five natural frequencies are listed in Table 3.

Figure 11 illustrates the computed natural oscillation shapes of the two models (1 and 2). Distinctions in their dynamic behavior become particularly visible at higher frequencies. The first mode, corresponding to a teetering seesaw, is a direct consequence of a single, constraint (clamp) along the middle line of the blade. While the second mode can be classified as dominantly pure bending, and all the higher modes demonstrate complex coupled bending-torsional behavior.

Table 3. Output parameters (characteristics) of the two models

Characteristic	Model 1	Model 2
Mass $m$ (kg)	0.5408	0.6084
Tip deflection $u_{tip}$ (mm)	6.7880	7.0370
1 <sup>st</sup> natural frequency (Hz)	1.1880	1.1350
2 <sup>nd</sup> natural frequency (Hz)	2.5050	2.3080
3 <sup>rd</sup> natural frequency (Hz)	5.5440	4.4260
4 <sup>th</sup> natural frequency (Hz)	5.5620	4.5540
5 <sup>th</sup> natural frequency (Hz)	5.8610	4.6060
Maximum failure criteria $I_{fail}$	0.6209	0.6511

## 7. CONCLUSIONS

The conducted research presents one possible approach to the conceptual design of a laminate blade structure through the use of multi-objective optimization procedure. Although the model is simple and number of design variables is not great, this engineering problem incorporates various research areas (e.g. aerodynamics, structural analysis, dynamic behavior, computation, optimization, etc.) and requires a multi-disciplinary approach and a robust optimization strategy. Aerodynamic performances of the designed wind turbine are estimated by CFD, i.e. by unsteady RANS equations closed by a two-equation  $k-\omega$  SST turbulence model. Computed transient aerodynamic forces acting on the blade are then used together with gravitational and inertial loads in the dimensioning of the structure in question. Through the integration of computational mechanics with a relatively novel heuristic optimization method, realized for both 2- and 3-criteria, sets of optimal solutions were determined and selected designs additionally investigated.

In order to make the best choice when aspects such as blade mass, amount and cost of used material, manufacturing process, etc. are of interest, simultaneous consideration of various, often opposing, aspects has to be performed. This paper also illustrates the comparison and individual assessment of the chosen optimal designs and justifies the application of a general mathematical model to a real engineering problem.

Demonstrated methodology could also be successfully applied to structures of greater dimensions as well as more complex geometries such as HAWT and propeller blades. Therefore, further work on this topic

involves more complex blade geometries or inner structures, a different collection of cost-functions and constraints or the use of another optimization method.

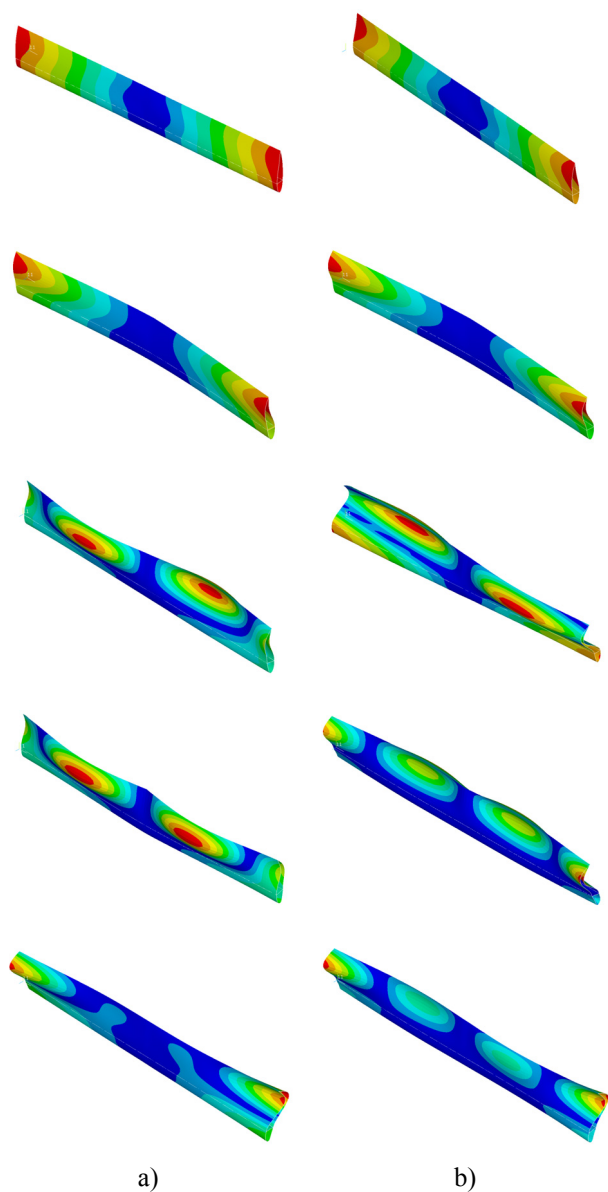


Figure 11. First five natural mode shapes of: a) model 1, b) model 2

#### ACKNOWLEDGMENT

The paper is a contribution to the research TR 35035 funded by the Ministry of Education, Science and Technological Development of the Republic of Serbia. It was also presented at YOUNG ResearcherS Conference, YOURS 2019, held in Belgrade, where it was chosen as one of the best papers and was awarded with the publication in the journal FME Transactions.

#### REFERENCES

- [1] Bottasso, C.L., Campagnolo, F. and Croce, A.: Multi-disciplinary constrained optimization of wind turbines, *Multibody System Dynamics*, Vol. 27, No. 1, pp. 21-53, 2012.
- [2] Forcier, L.C. and Joncas, S.: Development of a structural optimization strategy for the design of

next generation large thermoplastic wind turbine blades, *Structural and Multidisciplinary Optimization*, Vol. 45, No. 6, pp. 889-906, 2012.

- [3] Rašuo, B., Dinulović, M., Veg, A., Grbović, A. and Bengin A.: Harmonization of new wind turbine rotor blades development process: A review, *Renewable and Sustainable Energy Reviews*, Vol. 39, November, pp. 874-882, 2014.
- [4] Kavade, R.K. and Ghanegaonkar, P.M.: Effect of Best Position Blade Pitching on Power Coefficient of VAWT at Different Tip Speed Ratio by SST & DMST Model, *FME Transactions*, Vol. 46, No. 4, pp. 560-566, 2018.
- [5] Ivanov, T., Simonović, A., Svorcan, J. Peković, O.: VAWT Optimization Using Genetic Algorithm and CST Airfoil Parameterization, *FME Transactions*, Vol. 45, No. 1, pp. 26-31, 2017.
- [6] Ashuri, T., van Bussel, G. and Mieras, S.: Development and validation of a computational model for design analysis of a novel marine turbine, *Wind Energy*, Vol. 16, No. 1, pp. 77-90, 2013.
- [7] Raciti Castelli, M., Dal Monte, A., Quaresimin, M. and Benini, E.: Numerical evaluation of aerodynamic and inertial contributions to Darrieus wind turbine blade deformation, *Renewable Energy*, Vol. 51, March, pp. 101-112, 2013.
- [8] Albanesi, A., Bre, F., Fachinotti, V. and Gebhardt, C.: Simultaneous ply-order, ply-number and ply-drop optimization of laminate wind turbine blades using the inverse finite element method, *Composite Structures*, Vol. 184, January, pp. 894-903, 2018.
- [9] Fagan, E.M., De La Torre, O., Leen, S.B, Goggins, J.: Validation of the multi-objective structural optimisation of a composite wind turbine blade, *Composite Structures*, Vol. 204, November, pp. 567-577, 2018.
- [10] Wang, L., Kolios, A., Nishino, T., Delafin, P.-L. and Bird, T.: Structural optimisation of vertical-axis wind turbine composite blades based on finite element analysis and genetic algorithm, *Composite Structures*, Vol. 153, October, pp. 123-138, 2016.
- [11] Chen, J., Wang, Q., Shen, W.Z., Pang, X., Li, S. and Guo, X.: Structural optimization study of composite wind turbine blade, *Materials and Design*, Vol. 46, April, pp. 247-255, 2013.
- [12] Posteljnik, Z., Stupar, S., Svorcan, J., Peković, O. and Ivanov, T.: Multi-objective design optimization strategies for small-scale vertical-axis wind turbines, *Structural and Multidisciplinary Optimization*, Vol. 53, No. 2, pp. 277-290, 2016.
- [13] Garinis, D., Dinulović, M. and Rašuo, B.: Dynamic Analysis of Modified Composite Helicopter Blade, *FME Transactions*, Vol. 40, No. 2, pp. 63-68, 2012.
- [14] *ANSYS Fluent Theory Guide*, ANSYS, Inc., Canonsburg, Penn., 2017.
- [15] Menter, F.R.: Two-Equation Eddy-Viscosity Turbulence Models for Engineering Applications, *AIAA Journal*, Vol. 32, No. 8, pp. 1598-1605, 1994.

[16] Chowdhury, S., Tong, W., Messac, A. and Zhang, J.: A mixed-discrete particle swarm optimization algorithm with explicit diversity-preservation, *Structural and Multidisciplinary Optimization*, Vol. 47, No. 3, pp. 367-388, 2013.

---

**ВИШЕКРИТЕРИЈУМСКЕ ОГРАНИЧЕНЕ  
ОПТИМИЗАЦИЈЕ КОМПОЗИТНИХ ЛОПА-  
ТИЦА ВЕТРОТУРБИНА СА ВЕРТИКАЛНОМ  
ОСОМ ОБРТАЊА БАЗИРАНЕ НА КОНАЧНО-  
ЕЛЕМЕНТНОЈ АНАЛИЗИ И ОПТИМИЗАЦИЈИ  
БРОЈЕМ ЧЕСТИЦА**

**Ј. Сворцан, З. Тривковић, Т. Иванов, М. Балтић,  
О. Пековић**

Ветротурбине са вертикалном осом обртања представљају привлачно оруђе за искоришћење енергије ветра, нарочито погодно за мале потрошаче или неприступачне терене. Иако су једноставне геометрије (овде су претпостављене праве лопатице

константног аеропрофила), њихова аеродинамичка анализа може бити изразито сложена. Методе прорачунске механике флуида искоришћене су за процену аеродинамичких перформанси ротора. Рад даје преглед и оцену могућих стратегија за извршење вишекритеријумских оптимизација током пројектовања лопатице ветротурбине са вертикалном осом обртања ламинатне структуре које се односе на њене главне структурне параметре: редослед ређања и број слојева ламината. Бројни прорачуни структуре композитних лопатица ветротурбине изведени су методом коначних елемената. Вишекритеријумске ограничене оптимизације ројем честица, еволутивним методом, извршене су у односу на: укупну масу лопатице, највеће померање структуре лопатице при статичком оптерећењу, прорачунате сопствене фреквенције и критеријум лома по лопатици. Комбинацијом различитих улазних и излазних параметара (циљних функција и ограничења) могуће је дефинисати велики број прихватљивих, побољшаних решења.